JOURNAL OF Materials CHEMISTRY

Transformations of the low-dimensional zinc phosphates to complex open-framework structures. Part 2:† one-dimensional ladder to two- and three-dimensional structures

Amitava Choudhury,[a,b] S. Neeraj,[a] Srinivasan Natarajan[a] and C. N. R. Rao*[a,b]

[a]*Chemistry and Physics of Materials Unit, Jawaharlal Nehru Centre for Advanced Scientific Research, Jakkur P.O., Bangalore 560 064, India. E-mail: cnrrao@jncasr.ac.in*
[b]*Solid State and Structural Chemistry Unit, Indian Institute of Science, Bangalore 560 012, India*

Received 15th December 2000, Accepted 21st February 2001
First published as an Advance Article on the web 4th April 2001

Open-framework zinc phosphates with one-dimensional ladder structures are shown to transform, under simple reaction conditions, to two- and three-dimensional structures. Thus, the one-dimensional ladder, $[C_6N_4H_{22}]_{0.5}[Zn(HPO_4)_2]$, **I**, on heating with piperazine in aqueous solution gives a layer phosphate, $[C_4N_2H_{12}][Zn_2(PO_4)_2]$, **III**, and the three-dimensional phosphates $[C_2N_2H_{10}]_{0.5}[Zn(PO_4)]$, **IV**, $[C_6N_4H_{22}]_{0.5}[Zn_2(PO_4)_2]$, **V** and $[C_6N_4H_{21}]_4[Zn_{21}(PO_4)_{18}]$, **VI**. On heating in water in the absence of any amine, **I** transforms to a three-dimensional solid, $[C_6N_4H_{22}]_{0.5}[Zn_3(PO_4)_2(HPO_4)]$, **VII**, with 16-membered channels. Of these, **III** and **IV** are the only new compounds. The phosphates formed by the transformations of **I** exhibit unique structural features. Thus, in **III**, the layers are formed only with 3- and 4-membered rings and have step-like features due to the presence of infinite Zn–O–Zn linkages. Compound **IV** has a structure similar to that of the naturally occurring aluminosilicate, gismondine, and **VI** possesses unusual Zn_7O_6 clusters. The ladder zinc phosphate, $[C_3N_2H_{12}][Zn(HPO_4)_2]$, **II**, transforms to two layered compounds, $[C_3N_2H_{12}][Zn_4(PO_4)_2(HPO_4)_2]$, **VIII**, and $[C_3N_2H_{12}][Zn_2(HPO_4)_3]$, **IX**, on heating with zinc acetate and water, respectively. **II**, on heating in water in the presence of other amines, forms a ladder, $[C_3N_2H_5][Zn(HPO_4)]$, **X**, and a three-dimensional phosphate, $[C_3N_2H_{12}]_2[Zn_5(H_2O)(PO_4)_4(HPO_4)]$, **XI**. The syntheses and structures of **VIII–XI** have already been reported. What is interesting is that the majority of the transformations seem to occur through the process of deprotonation of the phosphoryl group and elimination of the $-HPO_4$ unit. The transformations of the ladder phosphates to higher dimensional structures reported in the present study not only demonstrate the seminal role of the one-dimensional structures as basic building units, but also the likely occurrence of self-assembly of these one-dimensional units in the building-up process.

Introduction

Zinc phosphates with open architectures have been investigated in great detail during the last decade.[1] Thus, zinc phosphates with zero-, one-, two- and three-dimensional structures have been prepared and characterized.[2–7] These compounds are, in general, synthesized by hydrothermal methods in the presence of organic amines. The presence of terminal –OH groups, particularly in the lower dimensional structures, prompted us to investigate the effect of deprotonation and the eventual transformations of these solids under hydrothermal conditions. Such a study assumes significance in the light of the recent suggestion that the complex three-dimensional open structures are likely to be formed through a progressive building up process, starting from low-dimensional structures.[8] The most important building unit or *synthon* of these structures in the zinc phosphate family appears to be the one-dimensional ladder structure along with the 4-membered ring monomer, whose transformations we have described elsewhere recently.[9b] With a view to investigating the transformations of one-dimensional structures to higher dimensional structures under appropriate conditions, we have taken up a detailed study of the transformations of two zinc phosphates, $[C_6N_4H_{22}]_{0.5}[Zn(HPO_4)_2]$, **I**,[5a] and $[C_3N_2H_{12}][Zn(HPO_4)_2]$, **II**,[3e] with one-dimensional ladder structures, synthesized in the presence of triethylenetetramine (TETA) and 1,3-diaminopropane (DAP) respectively. Interestingly **I** undergoes facile transformation under simple reaction conditions to yield two new compounds, $[C_4N_2H_{12}][Zn_2(PO_4)_2]$, **III**, and $[C_2N_2H_{10}]_{0.5}[Zn(PO_4)]$, **IV**, with layer and three-dimensional architectures respectively, besides three known three-dimensional open-framework zinc phosphates $[C_6N_4H_{22}]_{0.5}[Zn_2(PO_4)_2]$, **V**,[5a] $[C_6N_4H_{21}]_4[Zn_{21}(PO_4)_{18}]$, **VI**[9b] and $[C_6N_4H_{22}]_{0.5}[Zn_3(PO_4)_2(HPO_4)]$, **VII**.[5a] The other ladder phosphate, **II**, transforms to two layer phosphates $[C_3N_2H_{12}][Zn_4(PO_4)_2(HPO_4)_2]$, **VIII**[4b] and $[C_3N_2H_{12}][Zn_2(HPO_4)_3]$, **IX**,[2b] an unusual ladder compound with ligated amine, $[C_3N_2H_5][Zn(HPO_4)]$, **X**,[9b] and a three-dimensional phosphate, $[C_3N_2H_{12}]_2[Zn_5(H_2O)(PO_4)_4(HPO_4)]$, **XI**.[6e] The products **V–XI** are known compounds whose structures have been described adequately. The observation of the transformations of the one-dimensional ladder phosphates is of direct relevance to the mechanism of formation of the complex open-framework metal phosphates. We describe the transformations of **I** and **II** in this article, along with the structures of the new compounds obtained in the study.

Experimental

Synthesis and initial characterization

The one-dimensional zinc phosphates, $[C_6N_4H_{22}]_{0.5}[Zn(HPO_4)_2]$, **I**, and $[C_3N_2H_{12}][Zn(HPO_4)_2]$, **II**, were prepared

†Part 1 = reference 9*b*.

under hydrothermal conditions by using triethylenetetramine (TETA) and 1,3-diaminopropane (DAP), respectively.[5a,3e] Various experiments were performed starting with well-characterized crystals of **I** and **II**. Experimental parameters, such as the composition, the temperature as well as additives were varied in the different transformation experiments. The resulting products were single crystals in most cases, and were characterized by single crystal X-ray diffraction. The complete list of experimental parameters along with the products obtained in the transformation of the ladder compounds **I** and **II** are listed in Tables 1 and 2, respectively.

Single crystal X-ray diffraction

Suitable single crystals of each compound were carefully selected under a polarizing microscope and glued to a thin glass fiber with cyanoacrylate (super glue) adhesive. Single crystal structure determination by X-ray diffraction was performed on a Siemens Smart-CCD diffractometer equipped with a normal focus, 2.4 kW sealed tube X-ray source (MoKα radiation, $\lambda = 0.71073$ Å) operating at 50 kV and 40 mA. A hemisphere of intensity data was collected at room temperature in 1321 frames with ω scans (width of 0.30° and exposure time of 20 s per frame) in the 2θ range 3 to 46.5°.

The structures were solved by direct methods using SHELXS-86[10] and difference Fourier syntheses. An empirical absorption correction based on symmetry equivalent reflections was applied for all the compounds using the SADABS program.[11] All the hydrogen positions were initially located in the difference Fourier maps, and for the final refinement, the hydrogen atoms were placed geometrically and held in the riding mode. The last cycles of refinement included atomic positions for all the atoms, anisotropic thermal parameters for all non-hydrogen atoms and isotropic thermal parameters for all the hydrogen atoms. Full-matrix-least-squares structure refinement against $|F^2|$ was carried out using the SHELXTL-PLUS package of programs.[12] The lattice parameters of the various products obtained during the transformation reactions of **I** and **II** are listed in Table 3. Details of the final refinements of the two new zinc phosphates **III** and **IV** are presented in Table 4.

CCDC reference numbers 160294–160297, 151541, 160298, 151540, 160299–160301 and 151538. See http://www.rsc.org/suppdata/jm/b0/b010001n/ for crystallographic data in CIF or other electronic format.

Results

The ladder zinc phosphate, $[C_6N_4H_{22}]_{0.5}[Zn(HPO_4)_2]$, **I**, undergoes facile transformations to layer and three-dimensional structures in the presence of an additional amine under hydrothermal conditions. Thus, two new zinc phosphates, $[C_4N_2H_{12}][Zn_2(PO_4)_2]$, **III**, and $[C_2N_2H_{10}]_{0.5}[Zn(PO_4)]$, **IV**, with layer and three-dimensional structures respectively were obtained in the presence of piperazine. The ethylenediamine molecule found in **IV** was probably formed *in-situ* by the decomposition of the parent amine. In addition, **I** transforms readily into three-dimensional $[C_6N_4H_{22}]_{0.5}[Zn_2(PO_4)_2]$, **V**,[5a] and $[C_6N_4H_{21}]_4[Zn_{21}(PO_4)_{18}]$, **VI**,[9] on heating in the presence of piperazine or TETA, respectively, and to another three-dimensional phosphate, $[C_6N_4H_{22}]_{0.5}[Zn_3(PO_4)_2(HPO_4)]$, **VII**,[5a] on heating with water. While **IV**, **V** and **VI** possess 8-membered channels, **VII** has 16-membered channels (see Table 3). Layered zinc phosphates of known structures, $[C_3N_2H_{12}][Zn_4(PO_4)_2(HPO_4)_2]$, **VIII**,[4b] and $[C_3N_2H_{12}]$-$[Zn_2(HPO_4)_3]$, **IX**,[2b] were formed when **II** was heated with $Zn(OAc)_2$ and water, respectively. **II** also forms an unusual ladder compound, $[C_3N_2H_5][Zn(HPO_4)]$, **X**,[9b] and a three-dimensional compound, $[C_3N_2H_{12}]_2[Zn_5(H_2O)(PO_4)_4(HPO_4)]$, **XI**,[6e] on heating with other amines (see Table 2). Compounds **V–X** have been prepared independently by hydrothermal methods and their structures reported in the literature. We shall therefore not describe these structures here.

The layer structure **III** is unusual in that it is made-up of 3- and 4-membered rings with step-like features within the layers. The three-dimensional zinc phosphate, **IV**, with the 8-membered channel, has the structure of gismondine.[13] To our knowledge, both these structures are new and have been encountered for the first time, **IV** being the first pure zinc phosphate with the gismondine structure possessing an amine. The atomic coordinates of **III** are presented in Table 5. The asymmetric unit of **III** consists of 18 non-hydrogen atoms, 12 of which belong to the framework (comprising of two Zn, two P and eight O atoms) and six to the guest (two N, four C atoms) (Fig. 1). Two oxygen atoms are three-coordinated linking two Zn and one P atom (25% of the total oxygen atoms in the asymmetric unit) and the remaining have normal Zn–O–P links. The structure of **III** consists of a network of ZnO_4 and PO_4 moieties forming a layer with the inter-lamellar region occupied by the protonated amine. During the transformation,

Table 1 Experimental conditions for the transformation reactions of **I**

Composition **I**:Zn^{2+}:Amine:H_2O	Conditions			Product	Ref.
	T/°C	*t*/h	pH		
1:–:–:100	150	24	4	**VII**	5*a*
1:0.5:–:100	150	24	3.5	**VII**	5*a*
1:0.5:–:100	180	24	3.5	**VII**	5*a*
1:–:0.5 (PIP):100	150	24	10.5	**I**+**V**	5*a*
1:–:0.5 (PIP):200	150	24	10.5	**V**	5*a*
1:–:0.5 (PIP):100	165	24	10.5	**V**	5*a*
1:–:1 (PIP):100	150	24	>10.5	**V**	5*a*
1:–:1 (PIP):200	165	24	>10.5	**V**	5*a*
1:–:1 (PIP):100	165	24	>10.5	**V**	5*a*
1:–:1 (PIP):100	180	24	>10.5	**V**	5*a*
1:–:1.5 (PIP):100	150	24	>10.5	**III**+**V**	5*a*
1:–:1.5 (PIP):200	150	24	>10.5	**V**	5*a*
1:–:1.5 (PIP):200	165	24	>10.5	**IV**+**V**	GIS*, 5*a*
1:–:2 (PIP):100	150	24	>10.5	**III**+**VI**	Layer*, GIS*
1:–:2 (PIP):100	165	24	>10.5	**III**+**VI**	Layer*, GIS*
1:–:2 (PIP):100	165	36	>10.5	**III**+**VI**+**VI**	Layer*, GIS*, 9
1:–:2 (PIP):200	165	24	>10.5	**III**	Layer*
1:–:0.5 (TETA):100	150	24	6–7	**V**+**VI**	5*a*, 9
1:–:0.5 (TETA):100	165	24	—	**V**+**VI**	5*a*, 9
1:–:1 (TETA):100	150	24	—	**V**	5*a*

Source of Zn^{2+} ion was zinc acetate, TETA = triethylenetetramine, PIP = piperazine, GIS = gismondine, * = present work.

Table 2 Experimental conditions for the transformation reactions of **II**

Composition **II** : Zn^{2+} : Amine : H_2O	Conditions			Product	Ref.
	T/°C	*t*/h	pH		
1 : – : – : 100	85	48		**IX**	2*b*
1 : – : – : 100	110	24		**IX**	2*b*
1 : – : – : 100	150	24		**IX**	2*b*
1 : – : 0.9 (IM) : 20	100	48	6	**X** + **XI**	9, 6*e*
1 : – : 1.0 (MIM) : 20	100	48	7–8	**XI**	6*e*
1 : – : 0.67 (APY) : 20	100	48	6	**XI** + unidentified phase	6*e*
1 : – : 0.67 (HPIP) : 20	100	48	8–9	**XI**	6*e*
1 : – : 0.5 (BIPY) : 20	100	48	8	**XI**	6*e*
1 : – : 0.5 (GC) : 20	100	48	8	**XI** + unidentified phase	6*e*
1 : 0.5 $Zn(ac)_2$: – : 20	110	48	5–6	**IX** + **VIII** + unidentified phase + Hopeite	2*b*, 4*b*
1 : 0.5 $Co(ac)_2$: – : 20	110	48	5–6	**IX** + unidentified phase	2*b*
1 : 0.5 $Co(ac)_2$: – : 20	150	24		unidentified phase	
1 : 0.5 $CoCl_2 \cdot 6H_2O$: 20	110	48	5–6	**IX** + unidentified phase	2*b*

IM = Imidazole; MIM = 4-methylimidazole; APY = 3-aminopyridine; HPIP = homopiperazine; BIPY = 4,4′-bipyridine; GC = guanidinium carbonate.

the original amine (TETA) gets replaced by piperazine used for the deprotonation of the –OH groups.

The Zn atoms in **III** are all tetrahedrally coordinated with respect to oxygens with the Zn–O bond distances in the range 1.913(4)–2.005(3) Å [av. (Zn–O) = 1.956 Å]. The O–Zn–O bond angles are in the range 99.9(2)–121.4(2)° [av. (O–Zn–O) = 109.2°]. The longest bond distances and the largest bond angles are associated with the oxygen with trigonal coordination. The zinc atoms are connected to two distinct P atoms *via* Zn–O–P links with the average bond angles of 127.7°, resulting from a wide spread of angles. The two distinct P atoms, P(1) and P(2), are connected to Zn atoms *via* four P–O–Zn linkages. The P–O distances are in the range 1.517(4)–1.575(4) Å [av. (P–O) = 1.535 Å] and the O–P–O angles are in the 107.4(2)–112.2(2)° [av. (O–P–O) = 109.5°] range. The various geometrical parameters of **III** are in good agreement with those of other open-framework zinc phosphates.[2–9] The selected bond distances and angles are presented in Table 6. Assuming the usual valences for Zn, P and O, the framework stoichiometry of $Zn_2P_2O_8$ in **III** has a charge −2. The charge compensation is achieved by the presence of the doubly protonated piperazine molecule. This assignment is also consistent with the bond valence sum calculations.[14]

The framework structure of **III** consists of 3- and 4-membered rings formed by the vertex linkage between ZnO_4 and PO_4 tetrahedral units. The connectivity between these units is such that they form anionic layers and the piperazinium cations occupy the inter-lamellar voids. Thus, the entire structure can be considered to be made up of alternating anionic (inorganic) and cationic (organic) layers. The connectivity between the ZnO_4 and PO_4 units is such that it produces two distinct types of ladders made from 4- and 3-membered rings, respectively (A and B in Fig. 2). The presence of 3-membered rings connected edgewise forms infinite Zn–O–Zn linkages. The connectivity between A and B type ladders produces a layer with a step-like feature (Fig. 3). This type of layer with steps has been encountered recently in a zinc phosphate, $[NH_3(CH_2)_2NH(CH_2)_2NH_3]\cdot 2[Zn_2(PO_4)(HPO_4)]$.[6c] The formation of such steps can be explained by the presence of 3-membered ladders, which create strain in the layer, which is otherwise nearly planar.

The layered structure of **III** is stabilized by hydrogen bonding between the terminal P=O and the amine molecules as shown in Fig. 4. Layered zinc phosphates generally possess terminal P–OH units that interact with each other forming pseudo cavities wherein the amine molecules reside.[6c] In **III**, however, there are no terminal phosphoryl (P–OH) groups and the structural stability is provided by the interactions involving the amine molecule and terminal P=O groups (Fig. 4). The hydrogen bond interactions between the hydrogen atoms of the amine and the framework oxygens are given in Table 7. The coordination environment of the various sites in **III** merits some attention due to the unusual nature of the layer architecture. The circuit symbol, which enumerates the six distinct, smallest T atom loop pathways[15] (including the central atom itself), can be written as 4^46^2 or [4,4,4,4,6,6] for all tetrahedral atoms. Such a tetrahedral atom configuration has not been encountered in aluminosilicates or aluminophosphates. The circuit symbol is useful because it gives information on the local compactness of the net; thus the presence of many 3-, 4-, 5- and 6-circuits indicates compact building units, whereas 10- and 12-circuits are present in the circuit symbols of open nets with low-framework density. Thus, in **III**, both the Zn(1) and Zn(2) atoms are surrounded by two three-membered

Table 3 Lattice parameters for the compounds **I–XI**

Compound	Lattice parameters						Sp. grp.	Structure type	Ref.
	a/Å	*b*/Å	*c*/Å	*α*/°	*β*/°	*γ*/°			
I	5.267	13.302	14.783	90.0	96.049	90.0	$P2_1/c$	Ladder	5*a*
III	5.135	10.760	10.771	66.541	89.025	81.698	$P(-1)$	2D layer	*
IV	14.772	8.827	10.107	90.0	131.983	90.0	$C2/c$	3D (GIS topology)	*
V	8.064	8.457	9.023	111.9	108.0	103.6	$P(-1)$	3D (8R)	5*a*
VI	13.608	13.608	15.277	90.0	90.0	120.0	$R(-3)$	3D with cluster	9
VII	5.218	8.780	16.081	89.3	83.5	74.3	$P(-1)$	3D (16R)	5*a*
II	5.222	12.756	15.674	90.0	90.0	90.0	$P2_12_12_1$	Ladder	2*b* + 3*e*
VIII	17.279	5.193	20.115	90.0	92.61	90.0	$C2_1/c$	2D layer (tubular)	4*b*
IX	8.614	9.618	17.037	90.0	93.571	90.0	$P2_1/c$	2D layer (bifurcated 12R)	2*b*
X	5.197	7.697	17.336	90.0	90.618	90.0	$P2_1/c$	Ladder with bonded imidazole	9
XI	9.299	9.751	14.335	90.0	90.974	90.0	$P2_1$	3D (Interrupted THO topology)	6*e*

*Present work.

Table 4 Crystal data and struc0ture refinement parameters for $[C_2N_2H_{10}]_{0.5}[Zn(PO_4)]$, **III** and $[C_4N_2H_{12}][Zn_2(PO_4)_2]$, **IV**

Structural parameter	**III**	**IV**
Empirical formula	$Zn_2P_2O_8C_4N_2H_{12}$	$Zn_2P_2O_8C_4N_2H_{12}$
Crystal system	Triclinic	Monoclinic
Space group	$P(-1)$ (no.2)	$C2/c$ (no.15)
T/K	293	293
a/Å	5.1351(7)	14.7720(2)
b/Å	10.760(2)	8.8271(14)
c/Å	10.771(2)	10.1070(2)
α/°	66.541(2)	90.0
β/°	89.025(2)	131.983(2)
γ/°	81.698(2)	90.0
Volume/Å^3	539.70(13)	979.7(3)
Z	2	4
Formula mass	408.84	191.40
ρ_{calc}/g cm^{-3}	2.516	2.595
μ/mm^{-1}	4.778	5.254
θ range/°	2.06–23.26	2.96–23.32
Total data collected	2269	2024
Unique data	1520	711
Data [$I>2\sigma(I)$]	1168	554
R_{int}	0.029	0.060
R [$I>2\sigma(I)$]	$R_1=0.031$; $wR_2=0.069$[a]	$R_1=0.043$; $wR_2=0.096$[a]
R (all data)	$R_1=0.047$; $wR_2=0.076$	$R_1=0.059$; $wR_2=0.102$

[a] $W=1/[\sigma^2(F_o)^2+(aP)^2+bP]$ where $P=[F_o^2+2F_c^2]/3$; $a=0.0546$ and b = 0.0 for **III**, $a=0.0300$ and $b=0.0$ for **IV**.

Table 5 Atomic coordinates [$\times 10^4$] and equivalent isotropic displacement parameters [Å$^2\times 10^3$] for **III**, $[C_4N_2H_{12}][Zn_2(PO_4)_2]$

Atom	x	y	z	U(eq)[a]
Zn(1)	2931(1)	−26(1)	8560(1)	14(1)
Zn(2)	7906(1)	87(1)	6427(1)	14(1)
P(1)	6711(3)	1693(1)	3278(1)	12(1)
P(2)	−2732(3)	1749(2)	8307(1)	12(1)
O(1)	280(7)	1502(4)	8331(4)	22(1)
O(2)	3775(7)	−1503(4)	10299(4)	19(1)
O(3)	6221(7)	720(4)	7801(4)	17(1)
O(4)	1603(7)	−610(4)	7167(4)	17(1)
O(5)	7837(7)	1499(4)	4648(4)	20(1)
O(6)	6157(7)	−1449(4)	6673(4)	22(1)
O(7)	6876(8)	3124(4)	2228(4)	21(1)
O(8)	−3660(7)	3213(4)	7308(4)	21(1)
N(1)	1618(9)	4025(5)	6135(5)	21(1)
C(1)	1302(11)	3752(6)	4904(6)	24(1)
C(2)	1321(10)	5528(6)	5794(6)	18(1)
N(2)	1396(9)	3891(5)	1094(5)	27(1)
C(3)	1032(12)	3773(6)	−221(6)	29(2)
C(4)	1513(11)	5322(6)	894(6)	23(1)

[a] U(eq) is defined as one third of the trace of the orthogonalized U_{ij} tensor.

rings and two four-membered rings and makes five- and six-membered loops on either side of the central atom (Fig. 5a–d). The T-atom connectivity can be represented as [3,3,4,4,5,6] for both Zn(1) and Zn(2). Although, the loop configurations are identical for Zn(1) and Zn(2), it is to be noted that both of them are bonded into an eight-membered ring of neighboring TO_4 groups. The loop configurations for both P(1) and P(2) are similar, though identical to that of Zn(1) and Zn(2), however, is bonded into a seven membered ring of neighboring TO_4 groups (Fig. 5a,b). The coordination environment can also be represented in the Schläfli symbol, which specifies the connectivities of various vertex-linked polygons. The description of the various types of plane nets using the above symbolism has been discussed in detail by O'Keeffee and Hyde.[16] According to the Schläfli notation, the coordination environments of all the tetrahedral atoms (here Zn and P) are identical. Thus, for P(1) the environment can be represented as 3^24^2, meaning P(1) is surrounded by two triangles (three-membered rings) and two squares (four-membered rings).

Unlike **III**, compound **IV** possesses a three-dimensional structure closely resembling the aluminosilicate zeolite gismondine.[13] The atomic coordinates of **IV** are presented in Table 8. The asymmetric unit consists of 8 non-hydrogen atoms, 6 of which belong to the framework (comprising of one each of Zn and P and four O atoms) and two to the guest (one N and C atoms) (Fig. 6). All the oxygen atoms have normal Zn–O–P links. The structure of **IV** consists of a network of ZnO_4 and PO_4 forming channels that are occupied by the protonated amine. It is to be noted that the amine molecule of the original amine has been replaced by ethylenediamine.

Both the Zn and P are tetrahedrally coordinated with respect to the oxygens and the Zn–O bond distances vary in the 1.934(5)–1.963(5) Å range with an average value of 1.947 Å, in good agreement with the ZnO_4 tetrahedral units present in many zinc phosphates.[2–8] The O–Zn–O bond angles are in the range 96.7(2)–115.0(2)° [av. (O–Zn–O) = 109.3°]. The zinc atoms are connected to the P atom *via* four Zn–O–P links with the average bond angles of 131.7°. The P atom is also connected to Zn *via* four P–O–Zn linkages. The P–O distances range from 1.511(5)–1.545(5) Å (av. 1.536 Å) and the O–P–O angles are in the 107.9(3)–112.8(3)° [av. (O–P–O) = 109.5°] range. The various geometrical parameters observed for **IV** are in good agreement with other similar open-framework zinc phosphates.[2–9] The selected bond distances and angles are presented in Table 9. Assuming the usual valences for Zn, P and O, the framework stoichiometry of $ZnPO_4$ in **IV** has a charge −1. The charge compensation is achieved by the presence of half a molecule of the doubly protonated ethylenediamine molecule. This assignment is also consistent with the bond valence sum calculations.[14]

The structure of **IV** consists of a three-dimensionally connected framework of strictly alternating ZnO_4 and PO_4 tetrahedra. The tetrahedra are connected with one another by sharing the vertices to form four-membered rings that evolve into double-crankshaft chains along the c axis (Fig. 7). The double-crankshaft chains are cross-linked into an infinite three-dimensional framework bound by 8 T atoms (T = Zn, P) with channels along the [001] direction (Fig. 7). There are two distinct channels along the [001] and [111] directions (Figs. 7 and 8). These channels intersect to create the cages shown in Fig. 9a and b, in which the amine molecules are located. The hydrogen atoms of the amine molecule interact with the framework oxygen *via* hydrogen bond interactions (Table 7). The channels are elliptical in shape with the dimensions 5.1 × 8.1 Å [001] and 4.9 × 9.4 Å [111] (longest atom–atom contact distances, not including van der Waals radii). The "openness" of a structure is defined in terms of the tetrahedral atom density[13] (framework density, FD), defined as the number

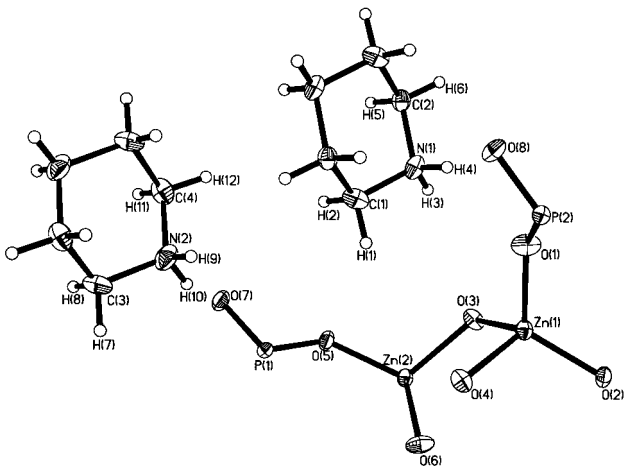

Fig. 1 ORTEP plot of the layered zinc phosphate, **III**, $[C_4N_2H_{12}][Zn_2(PO_4)_2]$. The asymmetric unit is labeled. Thermal ellipsoids are given at 50% probability.

Table 6 Selected bond distances and angles in **III**, $[C_4N_2H_{12}][Zn_2(PO_4)_2]$

Moiety	Distance/Å	Moiety	Angles/°	Moiety	Angles/°
Zn(1)–O(1)	1.913(4)	O(1)–Zn(1)–O(2)	121.4(2)	$O(6)^{\#2}$–P(1)–$O(4)^{\#2}$	107.9(2)
Zn(1)–O(2)	1.919(4)	O(1)–Zn(1)–O(3)	107.3(2)	$O(2)^{\#3}$–P(2)–O(8)	111.0(2)
Zn(1)–O(3)	1.997(3)	O(2)–Zn(1)–O(3)	109.0(2)	$O(2)^{\#3}$–P(2)–O(1)	112.2(2)
Zn(1)–O(4)	2.005(3)	O(1)–Zn(1)–O(4)	99.9(2)	O(8)–P(2)–O(1)	107.8(2)
Zn(2)–O(5)	1.911(4)	O(2)–Zn(1)–O(4)	113.6(2)	$O(2)^{\#3}$–P(2)–$O(3)^{\#4}$	108.1(2)
Zn(2)–O(6)	1.918(4)	O(3)–Zn(1)–O(4)	104.0(2)	O(8)–P(2)–$O(3)^{\#4}$	109.6(2)
Zn(2)–$O(4)^{\#1}$	1.992(3)	O(5)–Zn(2)–O(6)	118.1(2)	O(1)–P(2)–$O(3)^{\#4}$	108.1(2)
Zn(2)–O(3)	1.998(4)	O(5)–Zn(2)–$O(4)^{\#1}$	110.3(2)	P(2)–O(1)–Zn(1)	135.6(2)
P(1)–O(5)	1.517(4)	O(6)–Zn(2)–$O(4)^{\#1}$	108.6(2)	$P(2)^{\#3}$–O(2)–Zn(1)	132.1(2)
P(1)–O(7)	1.518(4)	O(5)–Zn(2)–O(3)	114.2(2)	$P(2)^{\#1}$–O(3)–Zn(1)	118.6(2)
P(1)–$O(6)^{\#2}$	1.530(4)	O(6)–Zn(2)–O(3)	101.5(2)	$P(2)^{\#1}$–O(3)–Zn(2)	125.3(2)
P(1)–$O(4)^{\#2}$	1.574(4)	$O(4)^{\#1}$–Zn(2)–O(3)	102.8(2)	Zn(1)–O(3)–Zn(2)	116.1(2)
P(2)–$O(2)^{\#3}$	1.519(4)	O(5)–P(1)–O(7)	111.0(2)	$P(1)^{\#2}$–O(4)–$Zn(2)^{\#4}$	118.4(2)
P(2)–O(8)	1.522(4)	O(5)–P(1)–$O(6)^{\#2}$	112.6(2)	$P(1)^{\#2}$–O(4)–Zn(1)	122.5(2)
P(2)–O(1)	1.530(4)	O(7)–P(1)–$O(6)^{\#2}$	108.6(2)	$Zn(2)^{\#4}$–O(4)–Zn(1)	118.8(2)
P(2)–$O(3)^{\#4}$	1.573(4)	O(5)–P(1)–$O(4)^{\#2}$	107.4(2)	P(1)–O(5)–Zn(2)	133.7(2)
		O(7)–P(1)–$O(4)^{\#2}$	109.2(2)	$P(1)^{\#2}$–O(6)–Zn(2)	135.3(2)

Organic Moiety

Moiety	Distance/Å	Moiety	Angles/°
N(1)–C(1)	1.483(7)	C(1)–N(1)–$C(2)^{\#5}$	111.2(4)
N(1)–C(2)	1.494(7)	N(1)–C(1)–$C(2)^{\#5}$	109.4(5)
$C(1)–C(2)^{\#5}$	1.500(7)	N(1)–C(2)–C(1)	111.3(4)
N(2)–C(4)	1.478(7)	C(4)–N(2)–C(3)	111.4(4)
N(2)–C(3)	1.489(7)	N(2)–C(3)–$C(4)^{\#6}$	107.3(5)
$C(3)–C(4)^{\#6}$	1.511(8)	N(2)–C(4)–$C(3)^{\#6}$	110.2(4)

Symmetry transformations used to generate equivalent atoms: #1 $x+1$, y, z; #2 $-x+1$, $-y$, $-z+1$; #3 $-x$, $-y$, $-z+2$; #4 $x-1$, y, z; #5 $-x$, $-y+1$, $-z+1$; #6 $-x$, $-y+1$, $-z$.

of tetrahedral (T) atoms per 1000 Å^3. In **IV**, the number of T atoms per 1000 Å^3 (here T = Zn and P) is 16.3. This is close to the FD value of gismondine (15.4), indicating that the structure of **IV** is indeed that of gismondine.

Discussion

Two new compounds, $[C_4N_2H_{12}][Zn_2(PO_4)_2]$, **III** and $[C_2N_2H_{10}]_{0.5}[Zn(PO_4)]$, **IV**, have been obtained in addition to the known $[C_6N_4H_{22}]_{0.5}[Zn_2(PO_4)_2]$, **V**, $[C_6N_4H_{21}]_4[Zn_{21}(PO_4)_{18}]$, **VI**, $[C_6N_4H_{22}]_{0.5}[Zn_3(PO_4)_2(HPO_4)]$, **VII**, $[C_3N_2H_{12}]$-$4(PO_4)_2(HPO_4)_2]$, **VIII**, $[C_3N_2H_{12}][Zn_2(HPO_4)_3]$, **IX**, $[C_3N_2H_5][Zn(HPO_4)]$, **X** and $[C_3N_2H_{12}]_2[Zn_5(H_2O)$-$(PO_4)_4(HPO_4)]$, **XI**, by the transformations of one-dimensional ladder zinc phosphates, $[C_6N_4H_{22}]_{0.5}[Zn(HPO_4)_2]$, **I**, and $[C_3N_2H_{12}][Zn(HPO_4)_2]$, **II**. The one-dimensional zinc phosphates themselves were prepared with two different amines, TETA and DAP, but they possess identical structures. While one of the compounds, **III**, formed by the transformation of the ladder phosphate **I** has a two-dimensional layer structure, the others, **IV**, **V**, **VI** and **VII**, exhibit three-dimensional architectures. The ladder phosphate **II** yields two layer phosphates **VIII** and **IX**, and a three-dimensional phosphate, **XI**. In addition, we also obtained **X**, which is a simple adduct of the ladder in **II** with the new amine added to effect the transformation. In all these transformations, deprotonation of the phosphoryl group and elimination of the $-HPO_4$ unit appear to be the common steps. In what follows, we examine these aspects in some detail.

The experimental conditions, especially the composition and temperature, have a profound effect on the transformations of **I** and **II**. A careful investigation of the experimental conditions indicates that there is a direct relation between the parent

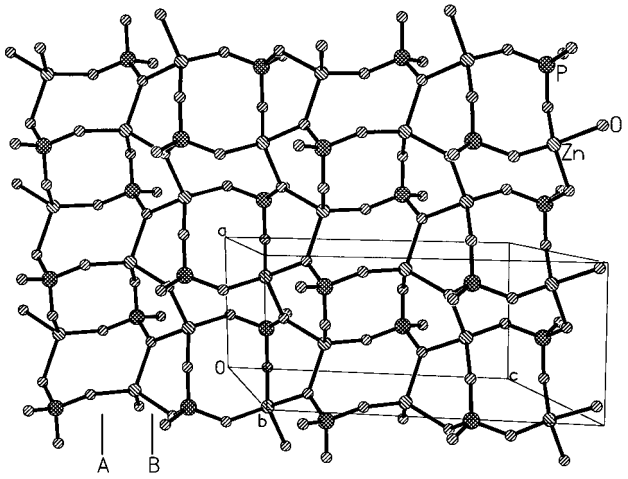

Fig. 2 Structure of **III** showing a single layer. Note the presence of two types of ladder arrangement marked A and B.

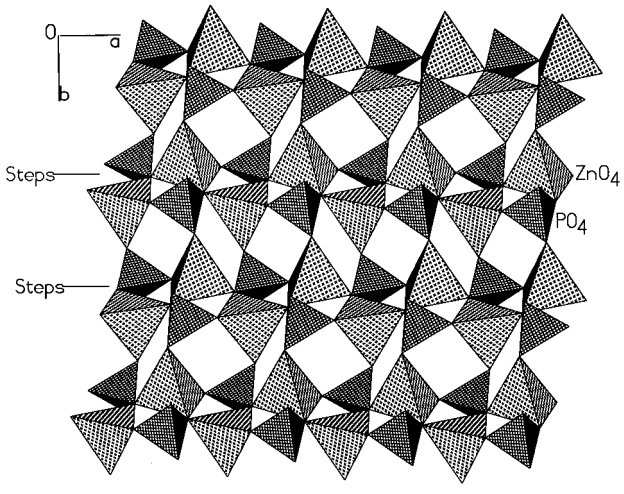

Fig. 3 Polyhedral view of **III** showing the step-like feature within the layer. The steps are created by the presence of 3-membered rings (see text).

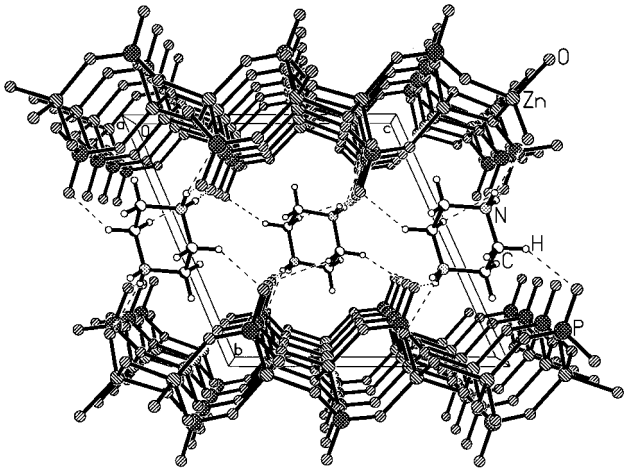

Fig. 4 Structure of **III** showing the layer arrangement. The amine molecules are situated in between the layers. Dotted lines represent the hydrogen bond interactions.

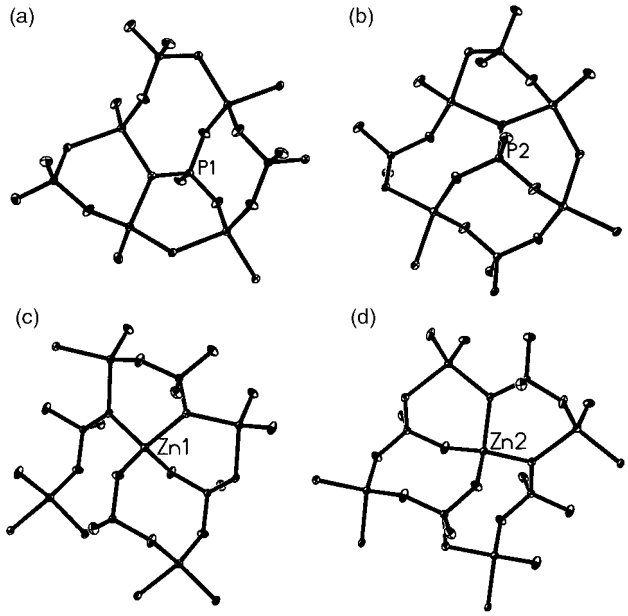

Fig. 5 Detail of the environment around P(1), P(2), Zn(1) and Zn(2). Note that both Zn(1) and Zn(2) are bonded to an eight-membered ring of neighboring TO_4 groups and the P(1) and P(2) to a seven-membered ring of neighboring TO_4 groups (see text).

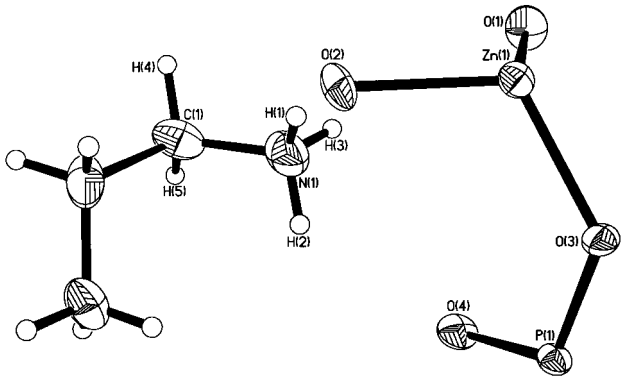

Fig. 6 ORTEP plot of the three-dimensional zinc phosphate, $[C_2N_2H_{10}]_{0.5}[Zn(PO_4)]$, **IV**. The asymmetric unit is labeled. Thermal ellipsoids are given at 50% probability.

ladder and the concentration of the amine (see Tables 1 and 2). As can be seen, during the transformation of **I** in the presence of an extra amine (piperazine, PIP), the predominant product is the three-dimensional zinc phosphate with 8-membered channels, $[C_6N_4H_{22}]_{0.5}[Zn_2(PO_4)_2]$, **V**, described recently.[5a] During these transformation, the amine molecule of the parent compound remains intact and the –OH group of the HPO_4 unit is completely deprotonated. On the other hand, when **I** is heated in water in the absence of any added amine, partial deprotonation occurs and **I** gets transformed into a three-dimensional zinc phosphate with 16-membered channels (Table 1).[5a] After a critical concentration of the amine (typically a pH of 10), compounds **III** and **IV** are formed, while in **III** the added amine, piperazine, not only deprotonates the –OH group from the HPO_4 units completely, but also replaces the amine molecule of the parent ladder, TETA, giving rise to a different architecture. **IV**, on the other hand, contains ethylenediamine, the amine molecule probably formed by the decomposition of the parent amine. Both **III** and **IV** contain phosphate groups, which are completely devoid of terminal –OH linkages. These observations are presented in Fig. 10 in the form of powder XRD patterns of the products with differing concentrations of PIP. As can be seen from the product phases, there is a competition between PIP and the parent amine (TETA) of the ladder resulting in a new product **III** (Fig. 10d and 10e), above a certain critical concentration of PIP (**I** : PIP = 1 : 1.5). It is to be noted that **III** contains PIP in between the layers rather than TETA, indicating that the parent amine has been replaced by the added amine. As mentioned earlier, when the concentration of the added PIP is low, **V** is the predominant product (Fig. 10b, 10c and Table 1). When the transformation is carried out in the presence of additional TETA (which is already present in **I** as part of the structure), a new three-dimensional zinc phosphate, $[C_6N_4H_{21}]_4[Zn_{21}(PO_4)_{18}]$, **VI**, possessing Zn_7O_6 clusters was

Table 7 Selected hydrogen bond interactions in compounds **III–IV**

Moiety	Distance/Å	Moiety	Angle/°
III			
O(2)···H(1)	1.919(9)	O(2)···H(1)–N(1)	158.1(4)
O(4)···H(2)	2.318(5)	O(4)···H(2)–N(1)	134.8(9)
O(3)···H(3)	2.070(5)	O(3)···H(3)–N(1)	145.6(9)
O(1)···H(4)	2.323(9)	O(1)···H(4)–C(1)	136.1(5)
IV			
O(8)···H(3)	1.734(6)	O(8)···H(3)–N(1)	166.8(7)
O(1)···H(4)	2.283(7)	O(1)···H(4)–N(1)	132.6(6)
O(8)···H(4)	2.230(6)	O(8)···H(4)–N(1)	154.1(5)
O(7)···H(9)	2.686(6)	O(7)···H(9)–N(2)	163.9(6)
O(7)···H(10)	2.137(6)	O(7)···H(10)–N(2)	150.7(6)
O(6)···H(10)	2.190(7)	O(6)···H(10)–N(2)	134.8(5)
O(8)···H(5)	2.556(7)	O(8)···H(5)–C(2)	138.2(6)
O(7)···H(6)	2.353(8)	O(7)···H(6)–C(4)	149.6(6)
O(7)···H(11)	2.546(7)	O(7)···H(11)–C(4)	130.3(6)
O(8)···H(12)	2.433(8)	O(8)···H(12)–N(4)	139.6(6)

Table 8 Atomic coordinates [$\times 10^4$] and equivalent isotropic displacement parameters [Å $\times 10^3$] for **IV**, $[C_2N_2H_{10}]_{0.5}[Zn(PO_4)]$

Atoms	*x*	*y*	*z*	*U*(eq)[a]
Zn(1)	3549(1)	8977(1)	−48(1)	16(1)
P(1)	3758(2)	11721(2)	−1895(2)	15(1)
O(1)	2039(4)	8101(6)	−2144(7)	25(1)
O(2)	4898(4)	7759(6)	607(6)	21(1)
O(3)	3493(4)	11064(5)	−770(7)	19(1)
O(4)	3557(4)	10511(6)	−3174(6)	21(1)
N(1)	3821(5)	7116(9)	−2854(9)	34(2)
C(1)	4306(7)	5844(10)	−3141(12)	35(2)

[a] *U*(eq) is defined as one third of the trace of the orthogonalized U_{ij} tensor.

Table 9 Selected bond distances and angles in **I**, $[C_2N_2H_{10}]_{0.5}[Zn(PO)_4]$

Moiety	Distance/Å	Moiety	Angles/°	Moiety	Angles/°
Zn(1)–O(1)	1.935(5)	O(1)–Zn(1)–O(4)$^{\#1}$	114.3(2)	O(3)–P(1)–O(4)	110.8(3)
Zn(1)–O(4)$^{\#1}$	1.940(5)	O(1)–Zn(1)–O(2)	108.6(2)	O(1)$^{\#2}$–P(1)–O(2)$^{\#3}$	108.2(3)
Zn(1)–O(2)	1.950(5)	O(4)$^{\#1}$–Zn(1)–O(2)	117.4(2)	O(3)–P(1)–O(2)$^{\#3}$	107.9(3)
Zn(1)–O(3)	1.963(5)	O(1)–Zn(1)–O(3)	103.7(2)	O(4)–P(1)–O(2)$^{\#3}$	109.3(3)
P(1)–O(1)$^{\#2}$	1.511(5)	O(4)$^{\#1}$–Zn(1)–O(3)	96.7(2)	P(1)$^{\#4}$–O(1)–Zn(1)	149.2(3)
P(1)–O(3)	1.542(5)	O(2)–Zn(1)–O(3)	115.0(2)	P(1)$^{\#3}$–O(2)–Zn(1)	124.6(3)
P(1)–O(4)	1.544(5)	O(1)$^{\#2}$–P(1)–O(3)	107.7(3)	P(1)–O(3)–Zn(1)	131.2(3)
P(1)–O(2)$^{\#3}$	1.545(5)	O(1)$^{\#2}$–P(1)–O(4)	112.8(3)	P(1)–O(4)–Zn(1)$^{\#5}$	121.9(3)
Organic Moiety					
Moiety	Distance/Å	Moiety	Angles/°		
N(1)–C(1)	1.462(11)	N(1)–C(1)–C(1)	113.0(6)		
C(1)–C(1)$^{\#6}$	1.53(2)				

metry transformations used to generate equivalent atoms: #1 x, $-y+2$, $z+1/2$; #2 $-x+1/2$, $y+1/2$, $-z-1/2$; #3 $-x+1$, $-y+2$, $-z$; #4 $-x+1/2$, $y-1/2$, $-z-1/2$; #5 x, $-y+2$, $z-1/2$; #6 $-x+1$, y, $-z-1/2$.

obtained,[9b] in addition to $[C_6N_4H_{22}]_{0.5}[Zn_2(PO_4)_2]$, **V**.[5a] During the formation of **VI**,[9] TETA undergoes a rearrangement forming a new amine molecule, tris-3-amino(ethylamine). Such a transformation of the amine molecule during the formation of open-framework phosphates has been reported.[17] **VII**, on the other hand, was formed by heating **I** in water, water acting as a mild base causing partial deprotonation. Thus, the crucial step in the transformation of **I** appears to be the deprotonation of the phosphoryl group, along with partial hydrolysis of the parent ladder. This argument gains strength from our observations of the transformation of the second ladder compound, $[C_3N_2H_{12}][Zn(HPO_4)_2]$, **II**.

When heated in water without any added amine, **II** is partially transformed into a layer structure, $[C_3N_2H_{12}][Zn_2(HPO_4)_3]$, **IX**,[2b] with the loss of one $-HPO_4$ group. **IX**, on the other hand, transforms into **II** when heated in water. This observation suggests that the two phases exist in equilibrium under experimental conditions and the transformations are facile and reversible. The transformations seem to occur over a wide temperature range of 85–150 °C. **II**, on heating with added amines, form a variety of products (Table 2), the predominant being a three-dimensional zinc phosphate with 8-membered channels, $[C_3N_2H_{12}]_2[Zn_5(H_2O)(PO_4)_4(HPO_4)]$, **XI**, with a thomsonite[13] related structure. This observation seems to suggest the occurrence of simultaneous deprotonation of the phosphoryl group (–OH) and condensation. The formation of $[C_3N_2H_5][Zn(HPO_4)]$, **X**, from **II** is interesting in that the amine molecule, imidazole, replaces the hanging $-HPO_4$ unit from the ladder structure. This indicates that the added amine (base), in addition to the deprotonation of the –OH group, also helps in the hydrolysis at the metal center. Such a process would bare the metal site and create opportunities for a nucleophilic type attack by other moieties present in the solution, during the hydrothermal transformation reactions. Our studies on the effect of the conjugate base of the acetic acid, $[(CH_3COO)^-]$, on the transformation of **I** and **II** were not conclusive. Although the acetate anion in solution is milder compared to the amines, proton abstraction from the phosphoryl group does indeed occur as evidenced from the products obtained (Tables 1 and 2).

The formation of the layered architectures **III**, **VIII** and **IX** can be visualized in terms of simple deprotonation and

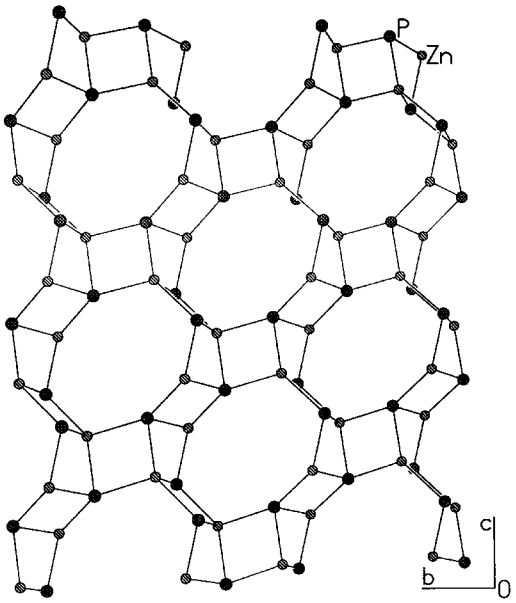

Fig. 7 The T-atom (T = Zn and P) connectivity along the c axis showing the 8-membered channels in **IV**. Note the presence of the crankshaft chains.

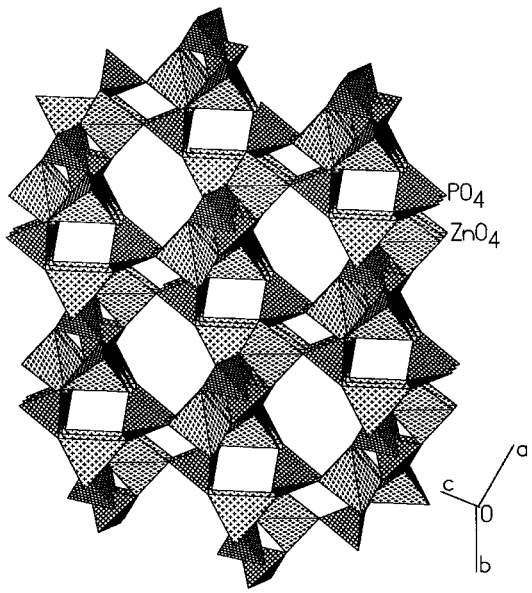

Fig. 8 Polyhedral connectivity in **IV** showing the 8-membered channels along the [111] direction.

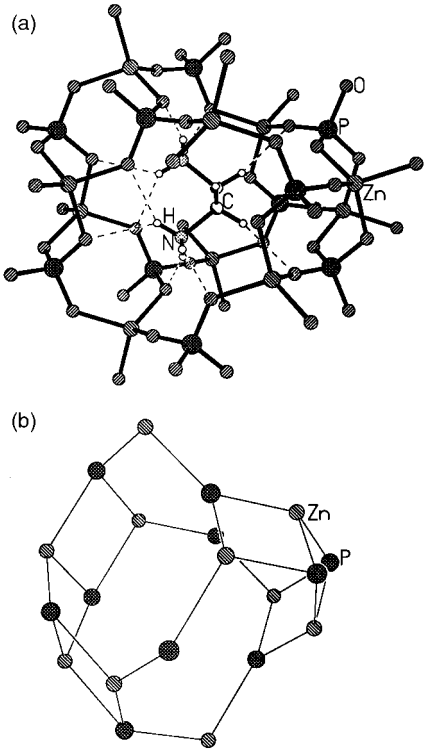

Fig. 9 Figure showing the cage-like cavity formed at the intersection between the two channels. (a) Ball and stick view showing the position of the amine and (b) T-atom connectivity. Dotted lines in (a) represent the possible hydrogen bond interactions.

elimination of phosphate from **I** and **II**, as shown below:

$$2[Zn(HPO_4)_2]\ (\mathbf{I}) \xrightarrow[-2HPO_4]{-2H^+} [Zn_2(PO_4)_2]\ (\mathbf{III}) \quad (1)$$

$$4[Zn(HPO_4)_2]\ (\mathbf{II}) \xrightarrow[-4HPO_4]{-2H^+} [Zn_4(PO_4)_2(HPO_4)_2]\ (\mathbf{VIII}) \quad (2)$$

$$2[Zn(HPO_4)_2]\ (\mathbf{II}) \xrightarrow{-HPO_4} [Zn_2(HPO_4)_3]\ (\mathbf{IX}) \quad (3)$$

Of these three layer compounds, **VIII** and **IX** have been obtained by the reaction of the parent ladder **II** with Zn(OAc) and water molecule, the acetate anions favoring the deprotonation of the $-HPO_4$ units. It is known that poly-condensation of phosphoric acid occurs through the deprotonation of the terminal –OH groups.[8] The deprotonation of the $-HPO_4$ units generally occurs in the presence of excess amine or acetate anions in the reaction mixture.[5a,6e] In the case of **III**, however, the parent amine molecule, TETA, present in the compound is replaced by the amine, PIP, added for deprotonation purposes, and in the process a new layered structure is produced. In all the newly formed compounds, the presence of the parent ladder structure can be clearly seen, as illustrated in Figs. 11–13.

A possible mechanism for the formation of **III** from **I** is shown in Fig. 11. In this reaction, two $-HPO_4$ units are eliminated from the parent ladder in addition to the deprotonation, accompanied by the insertion of the Zn^{2+} ion. Such a process gives rise to another ladder-like feature within the layer. **VIII** possesses linkages similar to **III**, but the connectivity between the two ladders gives rise to channel-like features within the layer.[4a] Accordingly, the connectivity between the pendent phosphates and Zn^{2+} (ZnO_4) in **VIII** is not planar but occurs above and below the plane of the ladder (Fig. 12). This is primarily responsible for the channel-like features within the layer. In **IX**, the ladders lose $-HPO_4$ groups and form a 12-membered aperture within the layer (Fig. 13). Thus, in all the layer compounds the parent signature of the ladder is present.

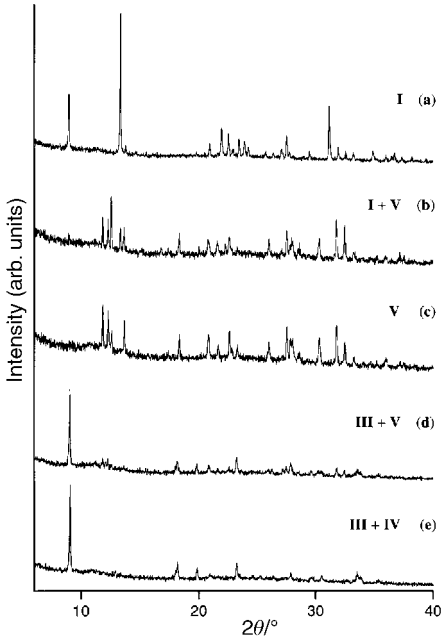

Fig. 10 Powder XRD patterns of the products obtained during the transformation of **I** with different molar ratios of PIP with respect to **I** (**I**:PIP) under similar conditions ($100H_2O$; 150 °C; 24 h) (a) 1:0.0PIP, (b) 1:0.5PIP, (c) 1:1.0PIP, (d) 1:1.5PIP and (e) 1:2.0PIP. (Also refer to Table 1.)

Compound **IV** is the only new three-dimensional structure obtained during the transformation reactions of the one-dimensional ladder. Again, the formation can be visualized in terms of deprotonation and elimination of a phosphate ion.

$$[Zn(HPO_4)_2]\ (\mathbf{I}) \xrightarrow[-HPO_4]{-H^+} [Zn(PO_4)]\ (\mathbf{IV}) \quad (4)$$

The gismondine structure of **IV** is constructed from crankshaft chains, which are nothing but 4-membered rings connected through their edges (ladders). As can be seen from Fig. 14, the ladders are connected through further 4-membered rings forming the 8-membered channels in **IV**. Similarly, the features of the ladder can be visualized in the three-dimensional structures of **V** and **VII** as well (Fig. 15). The three-dimensional structure, **XI**, obtained from **II** has the interrupted thomsonite structure, the building unit of which again contains ladder-like 4-membered rings.[6e] Thus, even in the three-dimensional structures the features of the starting structural motif, *viz.*, the ladder, are present, indicating that the one-dimensional

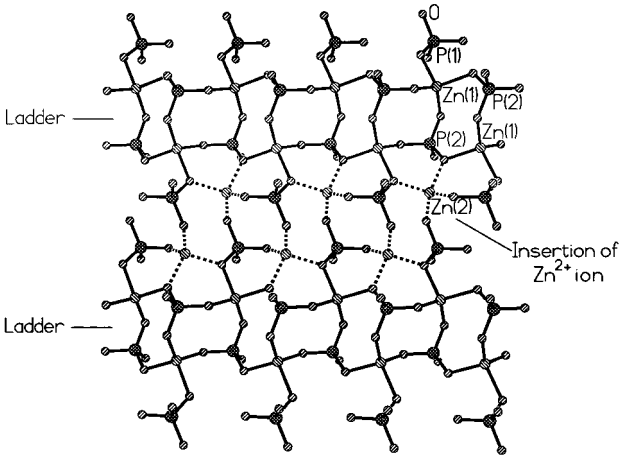

Fig. 11 A plausible schematic for the formation of the layer structure, **III**, from the ladder **I**. Note that the insertion of Zn^{2+} in between the ladders facilitates the formation of the layer.

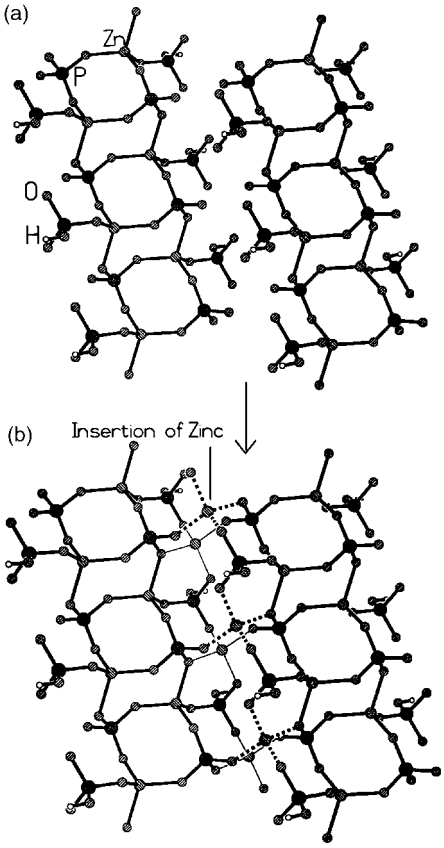

Fig. 12 Figure showing the schematic of formation of the layer structure, **V**, from the ladder **II**. Note the difference in connectivity between the ladders and Zn^{2+} (see Fig. 10 and text).

ladder is probably a basic building block in the formation of these open-framework phosphates. The presence of this motif in the complex two- and three-dimensional structures is also suggestive of the occurrence of self-assembly.

Conclusions

The transformations of one-dimensional ladder zinc phosphates to two- and three-dimensional structures have been investigated in detail. The present study constitutes one of the first attempts in understanding the formation of open-framework solids in the sense that the study attempts to experimentally demonstrate that there is a building-up process from low to higher dimensional structures. We are tempted to surmise that the one-dimensional ladder structure is a basic

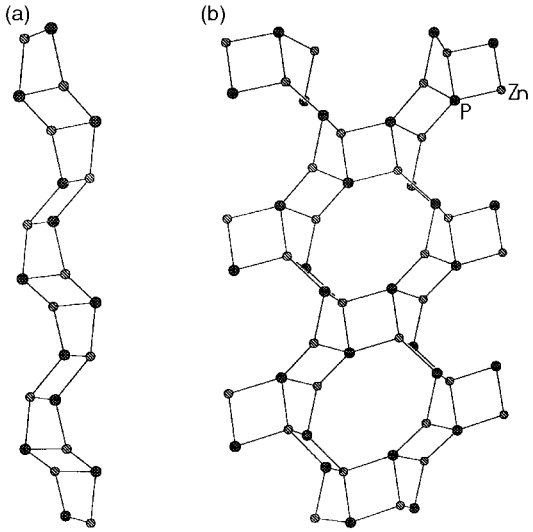

Fig. 14 Figure showing the double crankshaft chains (a) and their connectivity forming the channels in **IV**.

building unit of the complex zinc phosphates with open architectures. That the one-dimensional structure is likely to be a basic building block of these open-framework phosphates, is also supported by the recent observation of the transformation of a one-dimensional chain gallium phosphate by Walton *et al.*[18] to a three-dimensional structure. In this context, we should note that monomeric zinc phosphates have been isolated recently and these zero-dimensional structures also transform to one-, two- and three-dimensional structures.[9] What is interesting is that the structure of the zero-dimensional phosphates is nothing but a 4-membered ring with the composition $[Zn_2P_2O_4]$, and this 4-membered ring forms the one-dimensional ladder whose transformations have been investigated here. The present study of the transformation involves very simple chemical changes such as deprotonation of the phosphoryl (–OH) group and the subsequent condensation of the resultant phosphate moiety. The actual transformations of the one-dimensional ladder seem to involve self-assembly as evidenced from the presence of ladder-like features in the higher dimensional structures. Since such self-assembly is likely to occur spontaneously, it is not surprising that the low-dimensional structures are not as commonly found during the synthesis of open-framework materials.

It is necessary to continue such studies of transformation involving well-characterized low-dimensional structures. In this respect, *in-situ* X-ray diffraction studies would be most useful. It would be equally important to investigate reactions in

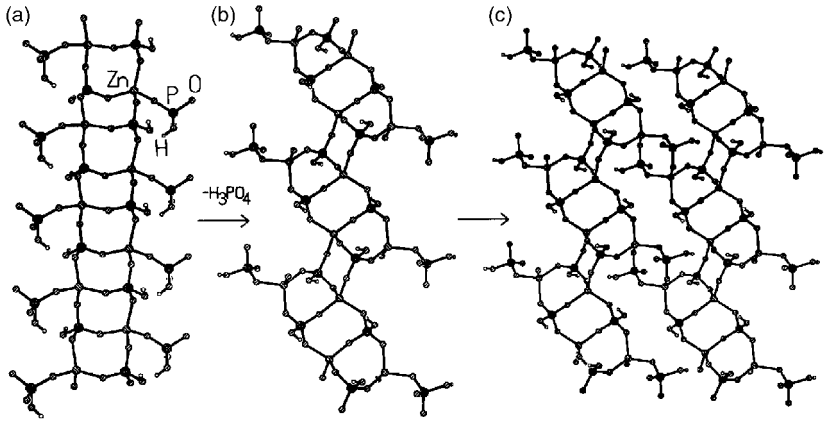

Fig. 13 (a–c) A possible mechanism for the formation of the layer structure **VI** from the ladder **II**. In (b) we show a possible intermediate (not isolated, yet).

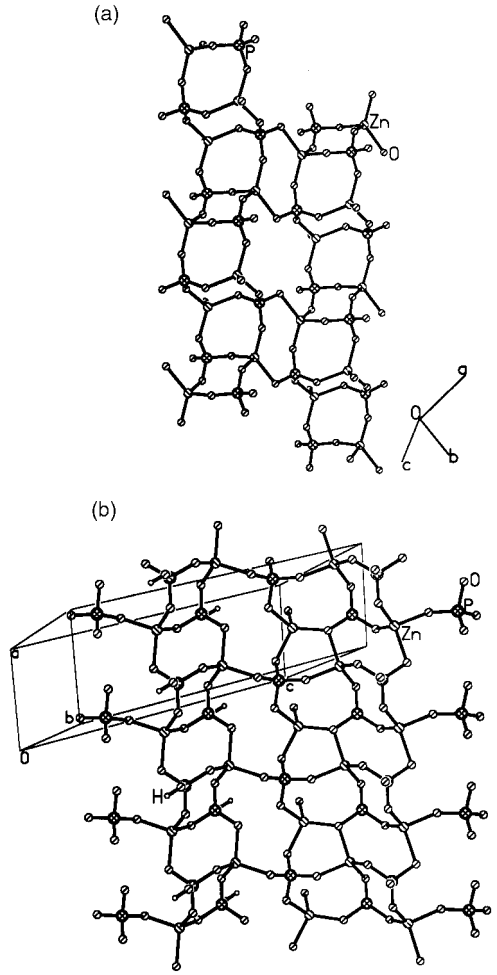

Fig. 15 (a) Structure of **V** along the *ab* plane. (b) Structure of **VII** along the *ac* plane. Note the presence of ladder-like features in both.

the solution state, particularly of the initial stages, by *in-situ* NMR measurements. Such solution NMR studies would be more feasible in the case of the transformations of the monomeric phosphates. With hindsight and a knowledge of the various intermediate species that have been isolated and characterized by single crystal methods, such *in-situ* investigations would prove invaluable.

References

1 A. K. Cheetham, T. Loiseau and G. Ferey, *Angew. Chem., Int. Ed.*, 1999, **38**, 3268.

2 (*a*) C. N. R. Rao, S. Natarajan and S. Neeraj, *J. Solid State Chem.*, 2000, **152**, 302; (*b*) S. Neeraj, S. Natarajan and C. N. R. Rao, *Angew. Chem., Int. Ed.*, 1999, **38**, 3480.

3 (*a*) J. Patarin, B. Marler and L. Huve, *Eur. J. Solid State Inorg. Chem.*, 1994, **31**, 909; (*b*) P. Reinert, N. Z. Logar, J. Patarin and V. Kaucic, *Eur. J. Solid State Inorg. Chem.*, 1998, **35**, 373; (*c*) W. T. A. Harrison, Z. Bircsak and L. Hannooman, *J. Solid State Chem.*, 1997, **134**, 148; (*d*) A. V. Chavez, T. M. Nenoff, L. Hannooman and W. T. A. Harrison, *J. Solid State Chem.*, 1999, **147**, 584; (*e*) W. T. A. Harrison, Z. Bircsak, L. Hannooman and Z. Zhang, *J. Solid State Chem.*, 1998, **136**, 93.

4 (*a*) D. Chidambaram, S. Neeraj, S. Natarajan and C. N. R. Rao, *J. Solid State Chem.*, 1999, **147**, 154; (*b*) S. Neeraj and S. Natarajan, *Int. J. Inorg. Mater.*, 1999, **1**, 317; (*c*) W. T. A. Harrison, M. L. F. Philips, W. Clegg and S. J. Teat, *J. Solid State Chem.*, 1999, **148**, 433, and references therein.

5 (*a*) A. Choudhury, S. Natarajan and C. N. R. Rao, *Inorg. Chem.*, 2000, **39**, 4295; (*b*) T. Song, M. B. Hursthouse, J. Chen, J. Xu, K. M. A. Malik, R. H. Jones, R. Xu and J. M. Thomas, *Adv. Mater.*, 1994, **6**, 679; (*c*) P. Feng, X. Bu and G. D. Stucky, *Angew. Chem., Int. Ed. Engl.*, 1995, **34**, 1745; (*d*) D. Chidambaram and S. Natarajan, *Mater. Res. Bull.*, 1998, **33**, 1275; (*e*) S. Neeraj, S. Natarajan and C. N. R. Rao, *Chem. Commun.*, 1999, 165; (*f*) G.-Y. Yang and S. C. Sevov, *J. Am. Chem. Soc.*, 1999, **121**, 8389.

6 (*a*) S. Neeraj, S. Natarajan and C. N. R. Rao, *New J. Chem.*, 1999, **23**, 303; (*b*) S. Neeraj, S. Natarajan and C. N. R. Rao, *J. Chem. Soc., Dalton Trans.*, 2000, 2499; (*c*) S. Neeraj, S. Natarajan and C. N. R. Rao, *Chem. Mater.*, 1999, **11**, 1390; (*d*) S. Natarajan, S. Neeraj and C. N. R. Rao, *Solid State Sci.*, 2000, **2**, 89; (*e*) S. Neeraj and S. Natarajan, *Chem. Mater.*, 2000, **12**, 2761.

7 C. N. R. Rao, S. Natarajan and S. Neeraj, *J. Am. Chem. Soc.*, 2000, **122**, 2810.

8 C. N. R. Rao, S. Natarajan, A. Choudhury, S. Neeraj and A. A. Ayi, *Acc. Chem. Res.*, 2000, **34**, 80.

9 (*a*) S. Neeraj, S. Natarajan and C. N. R. Rao, *J. Solid State Chem.*, 2000, **150**, 417; (*b*) A. A. Ayi, A. Choudhury, S. Natarajan, S. Neeraj and C. N. R. Rao, *J. Mater. Chem.*, 2001, **11**, 1181.

10 G. M. Sheldrick, *SHELXS-86 Program for Crystal Structure Determination*, University of Göttingen, Göttingen, Germany, 1986; G. M. Sheldrick, *Acta Crystallogr., Sect. A*, 1990, **35**, 467.

11 G. M. Sheldrick, *SADABS Siemens Area Detector Absorption Correction Program*, University of Göttingen, Göttingen, Germany, 1994.

12 G. M. Sheldrick, *SHELXS-93 Program for Crystal Structure Solution and Refinement*, University of Göttingen, Göttingen, Germany, 1993.

13 *Atlas of Zeolite Structure Types*, W. H. Meier and D. H. Olson (Eds.), Butterworth-Heineman, Boston, USA, 1992.

14 I. D. Brown and D. Aldermatt, *Acta Crystallogr., Sect. B*, 1984, **41**, 244.

15 (*a*) J. V. Smith, *Am. Mineral.*, 1977, **62**, 703; (*b*) J. V. Smith, *Chem. Rev.*, 1988, **88**, 149.

16 M. O'Keeffe and B. G. Hyde, *Philos. Trans. R. Soc. London A*, 1980, **295**, 553.

17 A. M. Chippindale, S. Natarajan, J. M. Thomas and R. H. Jones, *J. Solid State Chem.*, 1994, **111**, 18.

18 R. I. Walton, F. Millange, A. Le Bail, T. Loiseau, C. Serre, D. O'Hare and G. Ferey, *Chem. Commun.*, 2000, 203.